Interflavin Oxidation-Reduction Reactions between Pig Kidney General Acyl-CoA Dehydrogenase and Electron-Transferring Flavoprotein†

Robert J. Gorelick,‡ Lawrence M. Schopfer,§ David P. Ballou,§ Vincent Massey,§ and Colin Thorpe*,‡

Department of Chemistry, University of Delaware, Newark, Delaware 19716, and Department of Biological Chemistry, The University of Michigan, Ann Arbor, Michigan 48109

Received April 8, 1985

ABSTRACT: The mechanism of interflavin electron transfer between pig kidney general acyl-CoA dehydrogenase (GAD) and its physiological acceptor, electron-transferring flavoprotein (ETF), has been studied by static and stopped-flow absorbance and fluorescence measurements. At 3 °C, pH 7.6, reoxidation of the dehydrogenase (stoichiometrically reduced by octanoyl-CoA) by ETF is multiphasic, consisting of two rapid phases ($t_{1/2}$ of about 20 and 50 ms), a slower phase half-complete in about 1 s, and a final reaction with a half-time of 20 s. Only the two most rapid phases are significant in turnover. This complicated reaction course was dissected by examining the rates of plausible individual steps, e.g., GAD_{2e}·P + ETF_{1e}, GAD_{1e}·P + ETF_{ox}, and GAD_{1e}·P + ETF_{1e} (where P represents the product, octenoyl-CoA, and the subscripts indicate the redox state of the flavin). Rapid reaction and static fluorescence measurements, in all cases, showed that the final equilibrium mixture included appreciable levels of oxidized ETF. This was confirmed by measuring the reverse reactions, e.g., ETF_{1e} + GAD_{ox}·P, ETF_{1e} + GAD_{1e}·P, and ETF_{2e} + GAD_{ox}·P. These data support the following overall scheme for the reaction of GAD_{2e}·P with ETF_{ox}: The first and second phases correspond to reoxidation of GAD_{2e}·P in two successive one-electron steps requiring two molecules of ETF_{ox}. This results in a rapid rise in absorbance at 370 nm where the red anionic radicals of both product-complexed dehydrogenase and ETF absorb strongly. The slower decline in 370-nm absorbance reflects further reduction of ETF_{1e} by one- and two-electron-reduced forms of the product-complexed enzyme. In accord with the proposed scheme, the disproportionation of ETF semiquinone is catalyzed by the dehydrogenase in the presence of octenoyl-CoA, and this disproportionation reaction contributes to the attainment of the final equilibrium in the slower phases. In the absence of bound product, the reduction of ETF_{ox} by GAD_{2e} follows a different course, proceeding much more slowly to completion. Initial one-electron transfer generates the blue dehydrogenase semiquinone ($t_{1/2}$ = 600 ms at 3 °C) with concomitant formation of ETF red radical. Further reduction of ETF_{1e} proceeds very slowly ($t_{1/2}$ = 60 s), with concomitant reoxidation of the dehydrogenase radical. These data identify the important role played by acyl-CoA product in modulation of the thermodynamic and kinetic behavior of the dehydrogenase during the reoxidation of substrate-reduced enzyme by electron-transferring flavoprotein.

A group of soluble flavoprotein dehydrogenases found in the mitochondrial matrix passes electrons to the respiratory chain by a common, but unusual, path. In these reactions a hydride equivalent is passed from a saturated organic molecule to a flavoprotein dehydrogenase. The dehydrogenase then transfers its electrons via another flavoprotein, the electron-transferring flavoprotein (ETF)[1] (Crane & Beinert, 1956; Beinert, 1963a), to the membrane-bound iron–sulfur flavoprotein, ETF–ubiquinone oxidoreductase (Ruzicka & Beinert, 1977). The latter protein then reduces coenzyme Q, thus delivering electrons to the respiratory chain. This and a related pathway in certain anaerobic bacteria are the only known systems in which three flavoproteins are used sequentially in electron-transfer processes as shown:

substrates → primary flavoprotein dehydrogenases → ETF → ETF–ubiquinone oxidoreductase → CoQ

Thus, ETF services a variety of dehydrogenases. Three separate acyl-CoA dehydrogenases are involved in β-oxidation: one each for short, medium, and long-chain fatty acyl-CoA derivatives (Beinert, 1963b). Sarcosine and dimethylglycine dehydrogenases are involved in the degradation of choline (Beinert & Frisell, 1962; Frisell et al., 1966). Glutaryl-, isovaleryl-, and 2-methyl-branched-chain acyl-CoA dehydrogenases are involved in the catabolism of lysine, leucine, and isoleucine and valine, respectively (Besrat et al., 1969; Noda et al., 1980; Ikeda & Tanaka, 1983). Thus, the role of ETF includes both the general function of accepting electrons from a variety of dehydrogenases and the specific function of passing electrons to the membrane-bound ETF–dehydrogenase.

Despite several preliminary studies on the reactions between acyl-CoA dehydrogenases and ETF, the mechanism of this interflavin electron transfer remains poorly understood. No direct evidence has yet been obtained from static experiments for the existence of a complex between GAD and ETF, although steady-state and protein modification studies suggest

† This work was supported in part by grants from the U.S. Public Health Service (GM 11106 to V.M., GM 20877 to D.P.B., and GM 26643 to C.T.).

‡ University of Delaware.

§ The University of Michigan.

[1] Abbreviations: ETF, electron-transferring flavoprotein; ETF_{ox}, oxidized ETF; ETF_{1e}, semiquinone ETF; ETF_{2e}, fully reduced ETF; CoA, coenzyme A; GAD, general acyl-CoA dehydrogenase; GAD_{ox}, oxidized GAD; GAD_{ox}·P, oxidized GAD–octenoyl-CoA complex; GAD_{1e}·P, semiquinone GAD–octenoyl-CoA complex; GAD_{2e}·P, fully reduced GAD–octenoyl-CoA complex; GAD_{2e}, fully reduced GAD; EDTA, ethylenediaminetetraacetic acid; FAD, flavin adenine dinucleotide; Tris, tris(hydroxymethyl)aminomethane.

0006-2960/85/0424-6830$01.50/0

that their interaction is partly ionic (Frerman et al., 1980; Beckmann & Frerman, 1983).

On mixing equimolar ETF with GAD (reduced with octanoyl-CoA) in a stopped-flow spectrophotometer, Hall & Lambeth (1980) observed a rapid increase in absorbance at 375 nm which they ascribed to the formation of the red anionic state of ETF. This was followed by an approximately 10-fold slower loss of absorbance due to the formation of the fully reduced form of ETF. A similar reaction course was observed when ETF was reduced by catalytic levels of various dehydrogenases in the presence of excess substrate (Hall & Kamin, 1975; Reinsch et al., 1980; Beckmann et al., 1981; Steenkamp & Husain, 1982). Thus, it was clear that ETF_{1e} was formed first and then, in a slower process, was converted to the fully reduced form, ETF_{2e}. These reactions can be represented as

$$GAD_{2e}\cdot P + ETF_{ox} \rightarrow GAD_{1e}\cdot P + ETF_{1e}$$

$$GAD_{1e}\cdot P + ETF_{1e} \rightarrow GAD_{ox}\cdot P + ETF_{2e}$$

without prejudice to the protonation states of the various flavin species.

There are two difficulties with this hypothetical scheme. First, the second phase observed in these rapid reaction studies is too slow to be catalytically significant (Hall & Lambeth, 1980; Reinsch et al., 1980). Thus, the scheme depicted above would result in the accumulation of dehydrogenase radical unable to process another thio ester substrate until relieved of this second electron (Mizzer & Thorpe, 1981). Second, Hall & Lambeth (1980) were unable to specify the redox state of the dehydrogenase at the end of the fast phase. It is known that the dehydrogenase, in the absence of substrates, forms a blue neutral radical upon reduction with dithionite (Thorpe et al., 1979). However, in the initial stopped-flow study the expected blue neutral dehydrogenase radical (absorbing at 570 nm) was not observed at the end of the fast phase (Hall & Lambeth, 1980). Subsequent studies have found that in the presence of substrates and products, the red anionic semiquinone of GAD is thermodynamically stabilized (Mizzer & Thorpe, 1981), prompting the suggestion that the dehydrogenase radical might have escaped detection due to its spectral similarity to the corresponding ETF red anionic radical.

The present paper studies this reaction by examining directly the rate of electron transfer from either fully reduced- or radical forms of the dehydrogenase to either oxidized or semiquinone forms of ETF. It provides explanations for the failure to observe radical states of the dehydrogenase as noted earlier and shows that, in the presence of octenoyl-CoA, the overall reaction is actually quite close to equilibrium. Finally, this work demonstrates the profound influence exerted by octenoyl-CoA product bound to the reduced dehydrogenase on the interflavin redox reaction.

Materials and Methods

Materials. CoASH, lithium salt, and octanoyl-CoA were from P-L Biochemicals. Sodium dithionite was from Virginia Smelting Co., Portsmouth, VA. Amicon PM-30 ultrafiltration membranes were from Amicon. Sephacryl S-200 was purchased from Pharmacia. Trizma base was from Sigma. Ultrapure ammonium sulfate was obtained from Schwarz/Mann. *trans*-2-Octenoyl-CoA was prepared by the mixed anhydride procedure of Bernert & Sprecher (1977) and purified by chromatography on DE-52 (Lau et al., 1977) followed by desalting on a Bio-Gel P-2 column. Pig kidney ETF and general acyl-CoA dehydrogenase were purified according to the methods reported in Gorelick et al. (1982) with the following changes. In the dehydrogenase purification, the Matrex Gel-A step was substituted by gel filtration on a Sephacryl S-200 column, equilibrated with 20 mM phosphate buffer, pH 7.6. ETF was isolated from 4 kg of pig kidney cortex. The first dialysis step was extended from 12 to 96 h vs. 16 L of 5 mM Tris buffer, pH 8.5 at 4 °C, containing 5% v/v glycerol with one change after 48 h. The supernatant was then applied to a 5.0 × 90 cm DE-52 column equilibrated in 15 mM Tris buffer, pH 8.5 at 4 °C, with 5% v/v glycerol and then chromatographed on a 4.5 × 23 cm calcium phosphate gel–cellulose column as reported previously (Gorelick et al., 1982). The ETF was then concentrated by ultrafiltration on a PM-30 filtration membrane and applied to a 2.5 × 120 cm Sephacryl S-200 column equilibrated with 15 mM Tris buffer, pH 8.5 at 4 °C, with 5% v/v glycerol. These changes result in enzyme with A_{436}/A_{270} ratios of 5.9; no contaminants were seen on sodium dodecyl sulfate–polyacrylamide gel electrophoresis. Unless otherwise stated, all experiments described below were performed at 3 °C in 20 mM phosphate buffer, pH 7.6, containing 0.3 mM EDTA.

Anaerobic Techniques. Anaerobic experiments were performed by using all glass titration cuvettes and tonometers similar to those described by Williams et al. (1979). Protein samples were made anaerobic by repetitive cycles of evacuation with prepurified nitrogen scrubbed free of oxygen by passage over a column of Ridox catalyst (Fisher). Reagents were made anaerobic by bubbling for 15 min with oxygen-free nitrogen. Enzymes were photoreduced with 2.0 μM 3,10-dimethyl-5-deazaisoalloxazine or 3-methyllumiflavin and 6.0 mM EDTA by the method of Massey & Hemmerich (1978). The semiquinone general acyl-CoA dehydrogenase–octenoyl-CoA complex was prepared by the addition of octenoyl-CoA to oxidized acyl-CoA dehydrogenase and then photoreduced (see above).

Rapid Reaction Measurements. Transient kinetic measurements were made in a temperature-controlled, anaerobic stopped-flow spectrophotometer, interfaced to a Nova II (Data General Corp.) minicomputer system (Entsch et al., 1976; Beaty et al., 1981). When used in the spectral mode, this device was capable of recording spectra at 60 nm/s. For measurements above 530 nm, a Wratten filter no. 15 was inserted between the monochromator and the flow cell.

Fluorescence stopped-flow experiments were performed with a modified Gibson and Milnes spectrophotometer (Gibson & Milnes, 1964) using an observation cell based on the design of Gibson et al. (1966). Oxidized ETF was excited at 435 nm with emission at 500 nm. All measurements were performed at 3 °C.

Static Experiments. Absorbance titrations were performed on Cary 17, 118, or 219 double-beam recording spectrophotometers. The reference spectra used in this work are shown in Figure 1. Fluorescence titrations employed a ratio scanning spectrofluorometer designed and built by G. Ford and Dr. D. Ballou, as previously described (Moore et al., 1978). All measurements were made at 3 °C.

Data Analysis. The data were treated as a series of first-order processes. Thus, the Nova II computer was used to remove the slowest, apparent first-order phase from each time course, and this process was repeated until a single apparent first-order process remained. This procedure is analogous to standard methods for analysis of sequential first-order processes (Fersht, 1977).

Results and Discussion

Equilibrium between Octanoyl-CoA-Reduced General Acyl-CoA Dehydrogenase and ETF. When 10 μM ETF_{ox} was

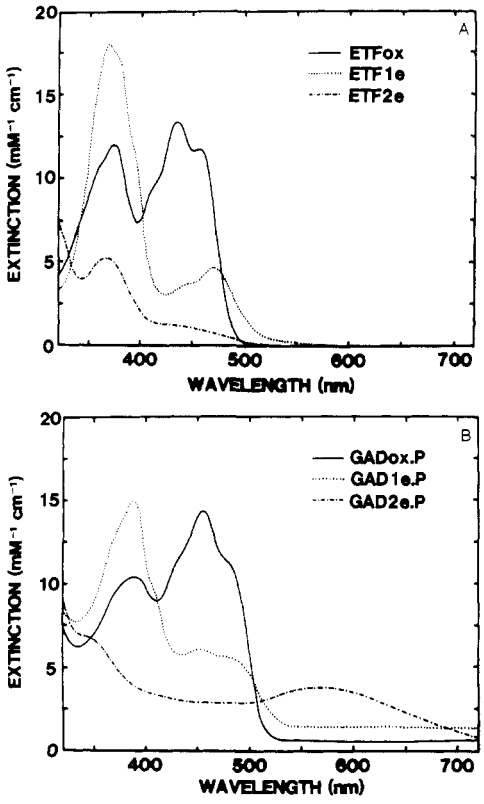

FIGURE 1: Reference spectra of pig kidney electron-transferring flavoprotein and general acyl-CoA dehydrogenase. The oxidized (—), semiquinone (···), and fully reduced (- - -) forms of electron-transferring flavoprotein (panel A) and general acyl-CoA dehydrogenase (panel B) are shown, in 20 mM phosphate buffer, pH 7.6 at 3 °C. Semiquinone forms of ETF and dehydrogenase and the reduced form of ETF were reduced by photoreduction as described under Materials and Methods. Fully reduced dehydrogenase was formed by the addition of excess substrate.

mixed with 5 μM octanoyl-CoA-reduced general acyl-CoA dehydrogenase (GAD_{2e}·P) in a stopped-flow spectrofluorometer, the characteristic fluorescence of ETF_{ox} decreased rapidly ($t_{1/2}$ of about 30 ms at 3 °C). However, considerable residual ETF_{ox} fluorescence remained under these conditions (data not shown), indicating that, in the presence of product, the redox potentials of the two couples are not far apart. The titration experiments shown in Figure 2 clearly demonstrate the characteristics of this equilibrium. In the experiment of panel A, a mixture of GAD_{ox} (10 μM) and ETF_{ox} (10 μM) was deoxygenated and titrated with octanoyl-CoA, a preferred substrate of the dehydrogenase (Thorpe et al., 1979). The progress of the titration was followed by absorbance and by the fluorescence of oxidized ETF (Gorelick et al., 1982). Note that after, 1 equiv of octanoyl-CoA had been added (in terms of dehydrogenase flavin), 28% of the oxidized ETF fluorescence still remained. Furthermore, absorbance changes at 570 nm, which are a measure of the characteristic reduced dehydrogenase–product charge-transfer complex (Thorpe et al., 1979), progressively accumulated from the onset of the titration. The shape of this long wavelength absorbance is clearly that of the substrate-reduced enzyme (Figure 1B). No ETF form absorbs at this wavelength (Figure 1A). It should be noted that, in the absence of ETF, in contrast to the above results, octanoyl-CoA effects almost stoichiometric reduction of the dehydrogenase (Thorpe et al., 1979).

When this experiment was repeated with dithionite as a titrant (in the absence of product; Figure 2, panel B), a different result emerged. The fluorescence of ETF_{ox} had completely disappeared after the addition of 10 μM dithionite.

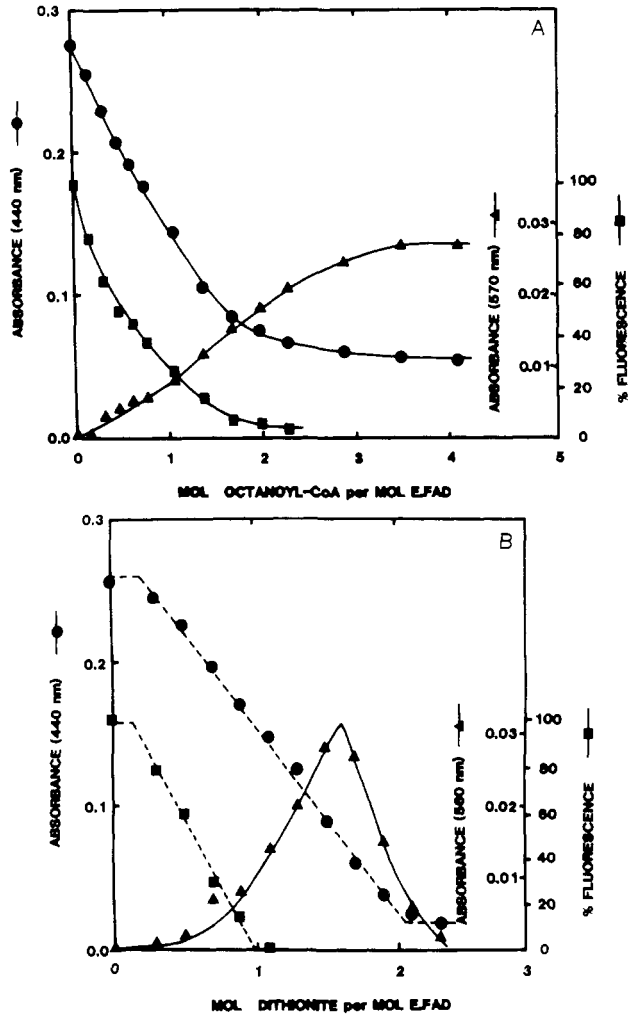

FIGURE 2: Titration of electron-transferring flavoprotein and general acyl-CoA dehydrogenase with either octanoyl-CoA or dithionite. ETF (10 μM) and dehydrogenase (10 μM) were mixed under anaerobic conditions in 20 mM phosphate buffer, pH 7.6, and 0.3 mM EDTA at 3 °C and titrated with either a deoxygenated solution of octanoyl-CoA (panel A) or dithionite (panel B). Absorbance measurements or percent fluorescence remaining are plotted vs. mole of titrant per mol total flavin. Fluorescence data were obtained by exciting at 435 nm and monitoring ETF_{ox} emission at 500 nm.

Further additions of dithionite then reduced the dehydrogenase to the dihydroflavin form, via the blue semiquinone as was seen in the absence of ETF (Thorpe et al., 1979). The measurements at 560 nm document this. This serial reduction, first of ETF_{ox} and then of the dehydrogenase, is expected from their respective redox potentials: ETF_{ox}/ETF_{2e} = −23 mV (Husain et al., 1984); GAD_{ox}/GAD_{2e} = −128 mV (Feinberg et al., 1982). However, in the presence of the product, octenoyl-CoA, it appears that the redox potential of the dehydrogenase becomes much closer to that of ETF and reducing equivalents are shared between both potential acceptors (Figure 2A). Thus, octenoyl-CoA modulates markedly the redox equilibrium between these two proteins. This shift in equilibrium between octanoyl-CoA-reduced dehydrogenase and ETF by octenoyl-CoA has not been previously documented and introduces a further complexity into the analysis of the interaction of these components.

Disproportionation of ETF Semiquinone Catalyzed by the General Acyl-CoA Dehydrogenase–Octenoyl-CoA Complex. ETF semiquinone disproportionates extremely slowly (e.g., $t_{1/2}$ = 10 h, 25 °C; Gorelick et al., 1982), and thus the significance of this reaction in catalysis has been discounted (Hall & Lambeth, 1980; Reinsch et al., 1980; Gorelick et al., 1982).

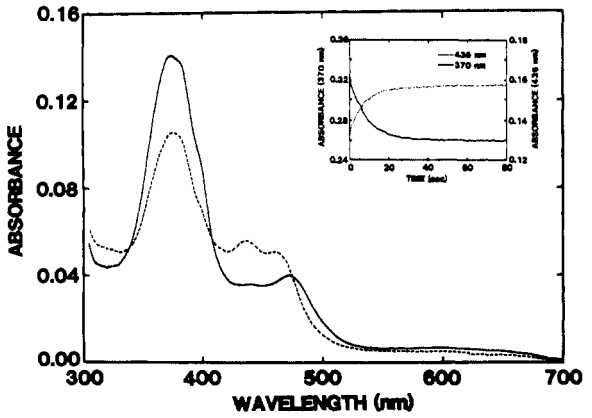

FIGURE 3: Disproportionation of ETF semiquinone catalyzed by general acyl-CoA dehydrogenase–octenoyl-CoA complex. ETF (8.6 μM) photoreduced to the semiquinone level (see Materials and Methods) in the presence of 50 μM octenoyl-CoA (—) in 20 mM phosphate, pH 7.6 at 25 °C, was mixed anaerobically with 0.1 μM dehydrogenase. The final equilibrium spectrum (- - -) was initiated 2 min after mixing. The recording speed was 2 nm/s. The inset shows absorbance vs. time traces when equal volumes of ETF semiquinone (20 μM), prepared as described above, and GAD_{ox}·P (2 μM; see Materials and Methods) were mixed at 3 °C, in a stopped-flow spectrophotometer employing a 2-cm path-length cell.

However, the experiments described above show that mixtures of dehydrogenase, octanoyl-CoA, and ETF are in redox equilibrium. Furthermore, this equilibrium is attained much more rapidly than the rates of disproportionation of ETF_{1e} alone. Thus, it appeared likely that mixtures of general acyl-CoA dehydrogenase and octenoyl-CoA would catalyze the disproportionation of ETF radical:

$$2ETF_{1e} \rightleftharpoons ETF_{2e} + ETF_{ox}$$

Accordingly, ETF semiquinone was prepared by photoreduction (see Materials and Methods) in the presence of octenoyl-CoA. As observed previously, disproportionation was very slow (Gorelick et al., 1982). The dehydrogenase ($^1/_{86}$ equiv) was then added from a sidearm. Figure 3 shows that the resulting spectral changes were consistent with disproportionation as observed previously (Gorelick et al., 1982). In the present case, however, the reaction was complete within 5 min. This experiment was repeated at a higher concentration of dehydrogenase ($^1/_{10}$ equiv) mixing 2 μM GAD_{ox}·P with 20 μM ETF_{1e} in a stopped-flow spectrophotometer. Changes in absorbance consistent with disproportionation were complete within 40 s (see inset Figure 3). This comparatively rapid, dehydrogenase-catalyzed disproportionation of ETF_{1e} probably contributes to the slower phases seen in these and previous rapid reaction studies. Indeed, disproportionation of ETF_{1e} is a necessary consequence of the overall mechanism which we propose for the transfer of electrons between GAD_{2e}·P and ETF (see Scheme I).

Scheme for Interaction of Octanoyl-CoA-Reduced GAD with Oxidized ETF. Scheme I depicts a plausible mechanism for electron transfer between substrate-reduced dehydrogenase and ETF_{ox}. We propose that the central diamond predominates in the normal catalytic sequence (see later). Turnover would be initiated by the reduction of the oxidized dehydrogenase by octanoyl-CoA (step 6). A suitable electron acceptor [e.g., 2,6-dichlorophenolindophenol in assays or ETF–dehydrogenase in vivo (Ruzicka & Beinert, 1977)] would accept electrons primarily from the ETF_{1e} (generated in steps 1 and 2) and thereby would allow continuous enzymatic turnover.

The reaction of 20 μM dehydrogenase with 24 μM octanoyl-CoA (step 6) was studied at 3 °C in the stopped-flow

Scheme I

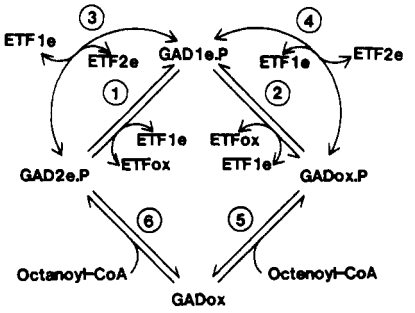

spectrophotometer. As observed by others, reduction of acyl-CoA dehydrogenase was multiphasic with a rapid phase accounting for a major portion of the changes seen (Hall et al., 1979; Reinsch et al., 1980; Ghisla, 1984). Under the conditions employed here, this rapid phase exhibited at $t_{1/2}$ of about 7 ms (data not shown).

On the basis of Scheme I, the primary route for reoxidation of substrate-reduced GAD would involve two one-electron steps (steps 1 and 2) to generate GAD_{ox}·P followed by dissociation of product (step 5). This sequence would reduce $2ETF_{ox}$ to $2ETF_{1e}$ and constitute the fast phase seen by Hall & Lambeth (1980). The two loops at the top of the scheme (steps 3 and 4) would account for the slower secondary changes. These steps would also be utilized in catalysis of the disproportionation of ETF_{1e} described above.

For clarity the redox couples of Scheme I are elaborated in four steps:

$$GAD_{2e}\text{·P} + ETF_{ox} \rightleftharpoons GAD_{1e}\text{·P} + ETF_{1e} \quad (1)$$

$$GAD_{1e}\text{·P} + ETF_{ox} \rightleftharpoons GAD_{ox}\text{·P} + ETF_{1e} \quad (2)$$

$$GAD_{2e}\text{·P} + ETF_{1e} \rightleftharpoons GAD_{1e}\text{·P} + ETF_{2e} \quad (3)$$

$$GAD_{1e}\text{·P} + ETF_{1e} \rightleftharpoons GAD_{ox}\text{·P} + ETF_{2e} \quad (4)$$

The first two reactions generate ETF semiquinone, whereas reactions 3 and 4 form dihydro-ETF. Notice that all steps shown involve one-electron transfers. Recent work with 5-deazaflavin-substituted dehydrogenase suggests that interflavin electron transfer to ETF involves obligatory one-electron steps (Gorelick & Thorpe, 1984). Thus, 1,5-dihydrodeaza-GAD is unable to reduce ETF at a measurable rate, although it is capable of rapidly reducing crotonyl-CoA to butyryl-CoA (Thorpe & Massey, 1983; Ghisla et al., 1984).

Analysis of the reactions of GAD_{2e}·P with ETF_{ox} measured using absorbance and fluorescence techniques is somewhat involved because of both the number of possible forms involved (at least six) and the high degree of spectral overlap between species (Figure 1). To assist in the analysis of the overall reaction of GAD_{2e}·P with ETF_{ox}, steps 1–4 were initiated separately and studied in both directions. This approach is feasible since GAD_{ox}·P, ETF_{ox}, GAD_{1e}·P, ETF_{1e}, GAD_{2e}·P, and ETF_{2e} forms can all be prepared separately in sufficient quantities to permit direct study of their interaction by rapid reaction techniques (see Materials and Methods).

Reaction of Octanoyl-CoA-Reduced General Acyl-CoA Dehydrogenase with Oxidized ETF (Step 1). Figure 4 shows absorbance traces obtained on mixing general acyl-CoA dehydrogenase, reduced by 1 equiv of octanoyl-CoA, with equimolar ETF_{ox} at 3 °C in a stopped-flow spectrophotometer. At 370 nm, a wavelength dominated by red semiquinone absorbance, an initial rapid rise in absorbance was seen ($t_{1/2}$ of about 30 ms) followed by a slower decline ($t_{1/2}$ of about 1 s). Finally, a very small absorbance decrease ($t_{1/2}$ of about 20 s)

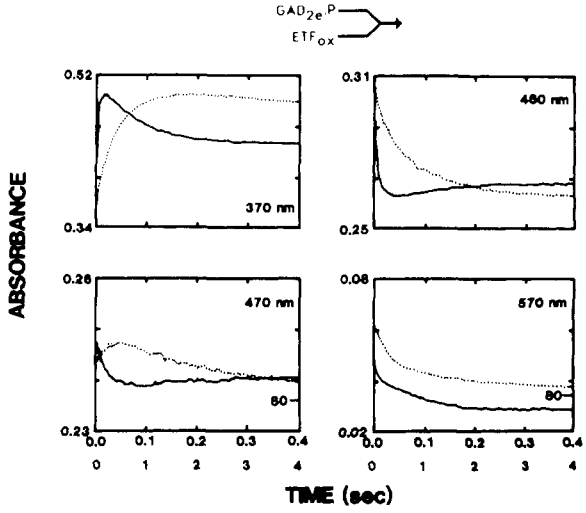

FIGURE 4: Absorbance vs. time traces following the reaction of fully reduced general acyl-CoA dehydrogenase–octenoyl-CoA complex with oxidized ETF. Oxidized GAD (20 μM) was reduced anaerobically with a stoichiometric amount of octanoyl-CoA to give GAD_{2e}·P. Equal volumes of GAD_{2e}·P (20 μM) and oxidized ETF (20 μM) were mixed in a stopped-flow spectrophotometer under anaerobic conditions, in 20 mM KP_i, pH 7.6 at 3 °C. In each panel, the traces display the absorbance changes over 0.4 (···) and 4.0 s (—) at the wavelength indicated. The mark labeled 80 indicates the final, stable absorbance after 80 s. Measurements were made in a 2-cm path-length cell.

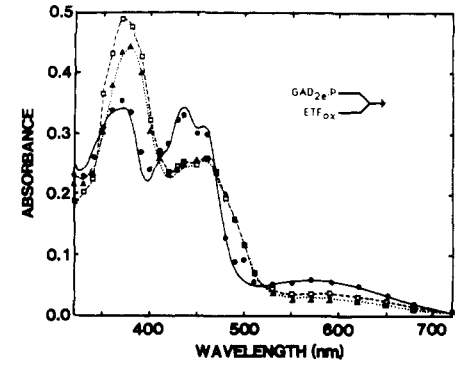

FIGURE 5: Spectra at selected times after initiation of a reaction between fully reduced general acyl-CoA dehydrogenase–octenoyl-CoA complex and oxidized ETF. Conditions are the same as in Figure 4. The dotted line is the final, stable spectrum, 2.5 min after initiation of the reaction. The solid line is the sum of the spectra of the reactants, taken before mixing. The circles indicate the zero time absorbances taken from the stopped-flow traces at each wavelength. Measurements were made relative to the final absorbances. The open squares indicate the absorbance 0.2 s after mixing, while the triangles show the absorbance at 4 s after mixing.

occurred over 80 s. Although not obvious, the rapid rise was biphasic. Hall & Lambeth (1980) also observed a rapid rise at 370 nm followed by a slower decrease but with correspondingly faster phases at 25 °C. A lower temperature was chosen for the present work in the hope of resolving intermediates occurring during the interaction of dehydrogenase with ETF and to facilitate the collection and interpretation of data.

Absorbance changes at 460 and 570 nm are also shown for this reaction in Figure 4. At 460 nm a rapid loss of absorbance ($t_{1/2}$ of about 30 ms) was followed by a small increase ($t_{1/2}$ of about 1 s) and, subsequently, a small decrease in absorbance ($t_{1/2}$ of about 20 s). At 570 nm, a rapid decrease in absorbance was followed by a slower decrease and a yet slower rise. When treated as a series of first-order processes, these absorbance changes could be resolved into four distinct kinetic events. The slowest absorbance change ($t_{1/2}$ of about 20 s) was monophasic, as was the next faster absorbance change ($t_{1/2}$ of about 1 s). The change that appeared over 200 ms was biphasic with $t_{1/2}$ of about 20 ms and $t_{1/2}$ of about 50 ms. This behavior was consistent throughout the wavelength range 320–650 nm. At 470 nm all four phases were visibly distinct, the direction of each successive phase being reversed (Figure 4). Though the absorbance changes at 470 nm were small and difficult to quantitate, they were reproducible from experiment to experiment and from one enzyme preparation to another. The biphasic nature of the rapid decrease in absorbance at 570 nm (0.4-s trace, Figure 4) can also be seen. Together, these observations argue strongly for the occurrence of two kinetic events during the rapid formation of semiquinone (over the first 0.4 s). We have assigned these rapid phases to steps 1 and 2 of Scheme I. The phase occurring with a $t_{1/2}$ of about 1 s has been assigned to a combination of steps 1–4, with the apparent rate being limited by steps 3 and 4. The slowest phase ($t_{1/2}$ of about 20 s) most likely represents a side reaction. These assignments will be discussed in greater detail later.

We have intentionally refrained from assigning rate constants to the above description for several reasons. First, since the reaction comes to an equilibrium state, any observed rate will consist of a combination of both forward and reverse microrates. Second, in view of the complexity of the reactions, it is not clear what combination of micro-rates should be used to fit a given observed rate. Third, the mechanistic complexities and the limited range of relative protein concentrations attainable practically are such that we have not been able to discriminate clearly between second-order kinetics and saturating first-order kinetics. Therefore, for simplicity, the phases have been characterized by times for half-completion ($t_{1/2}$) without implying that they represent true first-order processes.

In order to thoroughly characterize the spectral changes occurring upon the reaction of GAD_{2e}·P with ETF_{ox}, data were collected at multiple wavelengths over the spectral range 320–720 nm. This allowed us to construct spectra to illustrate the composition of the reaction mixture at strategic times during the reaction (Figure 5). Figure 5 shows the spectrum of the reaction times 0, 0.2, 4.0, and 150 s (the final, stable, equilibrium mixture) after mixing. The zero time spectrum is essentially coincident with the sum of the spectra of the reactants (Figure 5), indicating that no significant very rapid changes occurred during flow.

The spectrum at 0.2 s represents the reaction mixture at the end of the initial fast phase (steps 1 and 2). The spectrum is dominated by a peak at 370 nm, indicative of a substantial amount of red semiquinone. The rise in absorbance around 480 nm is also indicative of red semiquinone. In the 450-nm region, oxidized ETF absorbance has been lost, as expected. However, the sizable residual absorbance in this region indicates substantial oxidized flavin remaining. Fluorescence stopped-flow experiments (see earlier) indicated the loss of about 50% of the initial ETF_{ox} fluorescence during this phase. At long wavelengths, there is a general loss of absorbance consistent with oxidation of GAD_{2e}·P, but the changes are smaller than necessary for complete oxidation to either GAD_{1e}·P or GAD_{ox}·P. Attempts to quantitate the concentrations of the species contributing to this spectrum have been hampered by the number of components, the overlapping spectra, and our inability to independently constrain enough of the variables.

It is clear, however, on a qualitative level, that no significant amount of blue GAD_{1e}·P radical can be accommodated in the data. There was a continuous decrease in absorbance at wavelengths greater than 500 nm during the first 0.2 s of reaction. A significant involvement of blue radical would have

Table I: Extinction Coefficients[a] and Isosbestic Wavelengths for General Acyl-CoA Dehydrogenase and Electron-Transferring Flavoprotein

wavelength (nm)	GAD_{ox}·P	GAD_{1e}·P	GAD_{2e}·P	ETF_{ox}	ETF_{1e}	ETF_{2e}
326	6.6	7.9[b]	7.9[b]	4.8	3.6	6.4
331	6.3	7.8	7.3	5.4[b]	4.4	5.4[b]
333	6.2	7.8	7.2	5.9	4.8[b]	4.8[b]
342	6.5	8.1	6.9	7.5[b]	7.5[b]	4.0
348	6.8[b]	8.6	6.8[b]	8.5	10.0	4.1
370	9.3	12.7	5.1	11.7	18.1[c]	5.1
380	10.1	14.1	4.4	11.3	17.1	4.4
390	10.4	14.9	3.9	8.3	12.8	3.1
402	9.5	10.7	3.5	7.7[b]	7.7[b]	1.8
412	8.9[b]	8.9[b]	3.3	9.9	3.8	1.4
436	11.9	5.8	3.0	13.3[c]	3.5	1.2
440	12.3	5.8	3.0	13.1	3.5	1.1
446	13.4	5.9	2.9	12.0	3.6	1.1
450	14.1	6.0	2.9	11.6	3.7	1.0
460	13.9	5.9	2.9	11.6	4.1	0.9
470	12.1	5.6	2.8	8.1	4.6	0.7
480	11.4	5.6	2.9	4.3[b]	4.3[b]	0.6
500	5.4	4.6	2.8	0.2	1.6	0.2
503	4.2[b]	4.2[b]	2.8	0.1	1.4	0.1
507	2.9[b]	3.8	2.9[b]	0.1	1.1	0.1
513	1.5	3.0[b]	3.0[b]	0.1	0.8	0.0
560	0.6	1.4	3.8	0.0	0.0	0.0
570	0.6	1.4	3.8	0.0	0.0	0.0
650	0.6	1.4	2.3	0.0	0.0	0.0
692	0.5	1.3[b]	1.3[b]	0.0	0.0	0.0

[a] Extinction coefficients are in mM^{-1} cm^{-1}. [b] Isosbestic points between two species in the same row. [c] From Gorelick et al. (1982).

caused an increase in absorbance in this region, at least transiently. The absence of blue semiquinone was also noted by Hall & Lambeth (1980). However, formation of the blue dehydrogenase semiquinone is clearly evident when GAD_{2e}, prepared by photoreduction, is mixed with ETF_{ox} in the absence of product (see later). We therefore suggest that GAD_{1e}·P generated during this reaction must be predominantly the red anionic radical (Mizzer & Thorpe, 1981). A red GAD radical would be indistinguishable from a red ETF radical in our analysis.

Between 0.2 and 4.0 s, the major changes involve a loss of absorbance in the 370-nm region, indicative of the loss of semiquinone. Changes in the rest of the spectrum are minor, suggesting the formation of both fully oxidized and fully reduced flavins during this phase. We interpret these changes as a redistribution of electrons employing steps 3 and 4 to achieve an overall equilibrium involving all redox states of both GAD and ETF. The spectrum at 4.0 s clearly retains semiquinone character and the absorbance at long wavelength strongly suggests the presence of residual GAD_{2e}·P (Figure 5). Fluorescence data indicate the presence of ETF_{ox} at this point.

The steady-state turnover number extrapolated to saturating ETF levels is 1.6 s^{-1} under our experimental conditions (see Materials and Methods). Thus, the final slow phase, leading to a stable spectrum at about 80 s, cannot be involved in this turnover. To date, we have no satisfactory explanation for this phase. However, we have found that its amplitude (though not the rate of its appearance) varies depending upon the sample of ETF used. We have also noticed the appearance of a long wavelength absorbance in ETF_{1e} and ETF_{2e} during static dithionite titrations. The amplitude of this long wavelength absorbance varies from preparation to preparation in a manner that parallels its appearance in the stopped-flow experiments. We therefore suggest that this final kinetic phase is a secondary reaction, independent of electron transfer between GAD and ETF and is possibly associated with a long wavelength absorbing species in reduced ETF preparations.

Reaction of One-Electron-Reduced GAD-Octenoyl-CoA Complex with Oxidized ETF (Step 2). Figure 6 shows the time course of the reaction of GAD_{1e}·P with ETF_{ox} followed at several different wavelengths. At 480 nm, an isosbestic for the conversion of ETF_{ox} to ETF_{1e} (Figure 1; Table I), an initial rise in absorbance was seen reflecting the appearance of

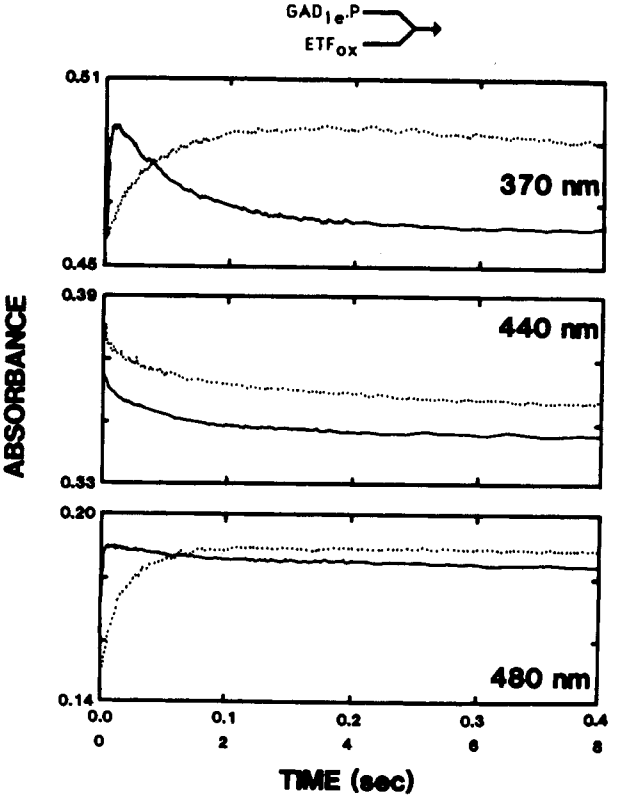

FIGURE 6: Absorbance vs. time traces following the reaction of the semiquinone general acyl-CoA dehydrogenase–octenoyl-CoA complex with oxidized ETF. GAD_{1e}·P was prepared as described under Materials and Methods. Equal volumes of GAD_{1e}·P (20 μM) and ETF_{ox} (20 μM) were mixed in a stopped-flow spectrophotometer under anaerobic conditions in 20 mM KP_i, pH 7.6, at 3 °C. In each panel, the time courses of the absorbance changes over 0.4 (···) and 8 s (—) are displayed. Measurements were made in a 2-cm path-length cell. The wavelength being monitored is indicated in each panel.

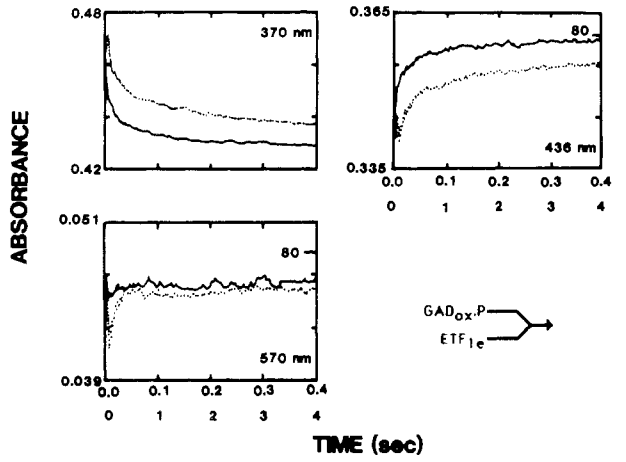

FIGURE 7: Absorbance vs. time traces following reaction of oxidized general acyl-CoA dehydrogenase–octenoyl-CoA complex and ETF semiquinone. ETF_{1e} and GAD_{ox}·P were prepared as described under Materials and Methods. Equal volumes of GAD_{ox}·P (20 μM) and ETF_{1e} (20 μM) were mixed in a stopped-flow spectrophotometer under anaerobic conditions in 20 mM KP_i, pH 7.6, at 3 °C. In each panel, the time courses of the absorbance changes over 0.4 (···) and 4 s (—) are displayed. The mark labeled 80 indicates the final absorbance, after 80 s. Measurements were made in a 2-cm path-length cell. The wavelength being monitored is indicated in each panel.

GAD_{ox}·P. This was followed by a small loss of absorbance. There was no indication of the very slow phase at any wavelength for this reaction. At 370 nm, the positive extinction coefficient change of ETF_{ox}/ETF_{1e} is greater than the corresponding negative extinction change of GAD_{1e}·P/GAD_{ox}·P; thus, a fast initial rise was observed. This was followed by a loss of absorbance back to the initial position during the final reequilibration phase. Similarly, an increased absorbance was seen at 503 nm (a wavelength where GAD_{1e}·P and GAD_{ox}·P are isosbestic, Figure 1; Table I), reflecting an increase in red semiquinone due to ETF_{1e} (data not shown). This was in turn followed by a small loss in absorbance. At 570 nm (not shown) small losses in absorbance were seen in both phases, consistent with conversion of GAD_{1e}·P to GAD_{ox}·P with, at most, minor amounts of GAD_{2e}·P being formed. At 440 nm (Figure 6) a biphasic decrease in absorbance indicated a net loss of oxidized flavin in both phases.

When treated as a series of first-order reactions, the absorbance changes at all wavelengths showed only two phases with $t_{1/2}$ of about 35 ms for the fast phase and $t_{1/2}$ of about 1 s for the slow phases. The absorbance changes in the fast phase indicate the dominant reaction to be step 2, equilibration between GAD_{1e}·P/GAD_{ox}·P and ETF_{ox}/ETF_{1e} (see eq 1). Contribution from step 1 cannot be excluded as ETF_{1e} is formed, but the net effect favors step 2. The half-time for this rapid step (35 ms) is similar to those assigned earlier to steps 1 and 2 (20–50 ms).

The slow phase ($t_{1/2}$ of about 1 s) is comparable to the middle phase seen when GAD_{2e}·P was reacted with ETF_{ox}. As in that case, the absorbance changes indicate a general redistribution of electrons to a final equilibrium position. This redistribution involves a loss of semiquinone, as evidenced by the decrease in absorbance at 370 nm, and a net loss of oxidized species, as indicated by the decrease in absorbance at 440 nm. That implies that GAD_{2e}·P and ETF_{2e} are formed. However, formation of GAD_{2e}·P must be significantly less than the conversion of GAD_{1e}·P to GAD_{ox}·P, since the net changes in absorbance at 570 nm are down.

Reaction of ETF Semiquinone with Oxidized GAD–Octenoyl-CoA Complex (Step 2). For the model in Scheme I to be internally consistent, the reaction of GAD_{ox}·P with ETF_{1e}

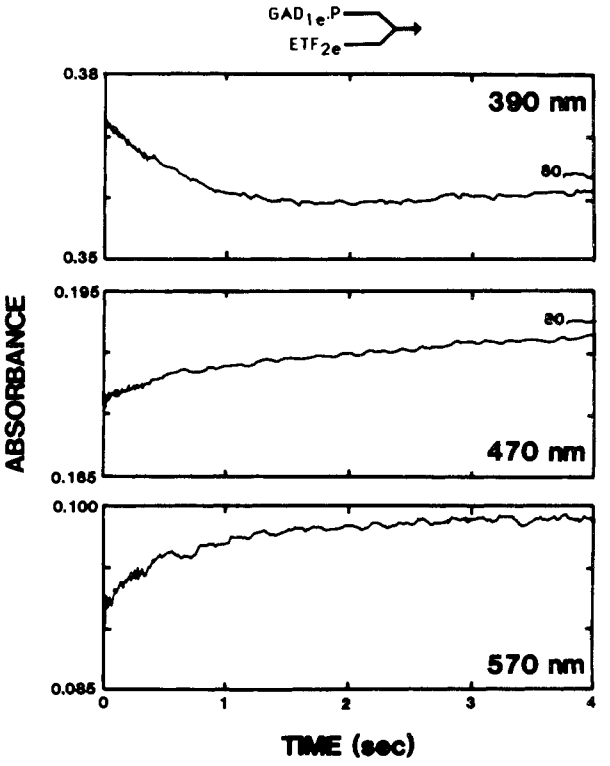

FIGURE 8: Absorbance vs. time traces following the reaction of semiquinone general acyl-CoA dehydrogenase–octenoyl-CoA complex with fully reduced ETF. GAD_{1e}·P and ETF_{2e} were prepared as described under Materials and Methods. Equal volumes of GAD_{1e}·P (20 μM) and ETF_{2e} (20 μM) were mixed in a stopped-flow spectrophotometer under anaerobic conditions in 20 mM KP_i, pH 7.6, at 3 °C. In each panel, the time course of the absorbance changes over 4 s is displayed. The mark labeled 80 indicates the final absorbance, after 80 s. Measurements were made in a 2-cm path-length cell. The wavelength being monitored is indicated in each panel.

would be expected to show two rapid phases at rates comparable to steps 1 and 2, followed by a slower phase as was found when GAD_{2e}·P was reacted with ETF_{ox}. In fact, this is the case. Figure 7 illustrates the time courses of the reaction when equimolar amounts of GAD_{ox}·P and ETF_{1e} were mixed in the stopped-flow spectrophotometer. At 370 nm, there was a triphasic loss of absorbance indicating a net loss of semiquinone in all phases. At 436 nm, there was a net gain in absorbance throughout all phases, reflecting a net gain in oxidized species overall. A rise in absorbance at 570 nm during the first 100 ms suggests the rapid formation of reduced GAD forms. Analysis of the traces as sequential first-order reactions, revealed phases with $t_{1/2}$ values of 20 ms, 50 ms, and 1 s. The agreement of these values with those reported in an earlier section for the reaction of GAD_{2e}·P with ETF_{ox} is consistent with our proposal (Scheme I) for a pair of rapid one-electron transfers in that reaction. Subsequent redistribution of electrons to generate a final equilibrium including ETF_{2e} occurs at a much slower rate. In the reaction under discussion, the secondary redistribution of electrons can be viewed as a catalyzed disproportionation of flavin radical species. By successively implementing either steps 1 and 3 or steps 2 and 4, it is possible to convert $2ETF_{1e}$ into ETF_{2e} and ETF_{ox} with no net change in the GAD species.

Reaction of Octenoyl-CoA Complexes of Oxidized, Semiquinone, and Fully Reduced Forms of GAD with ETF in Different Oxidation States (Steps 3 and 4). Scheme I also requires demonstration that steps 3 and 4 are consistent with $t_{1/2}$ values of about 1 s. Figure 8 shows the time course of the reaction of GAD_{1e}·P with ETF_{2e} (step 3), at 570, 470, and 390

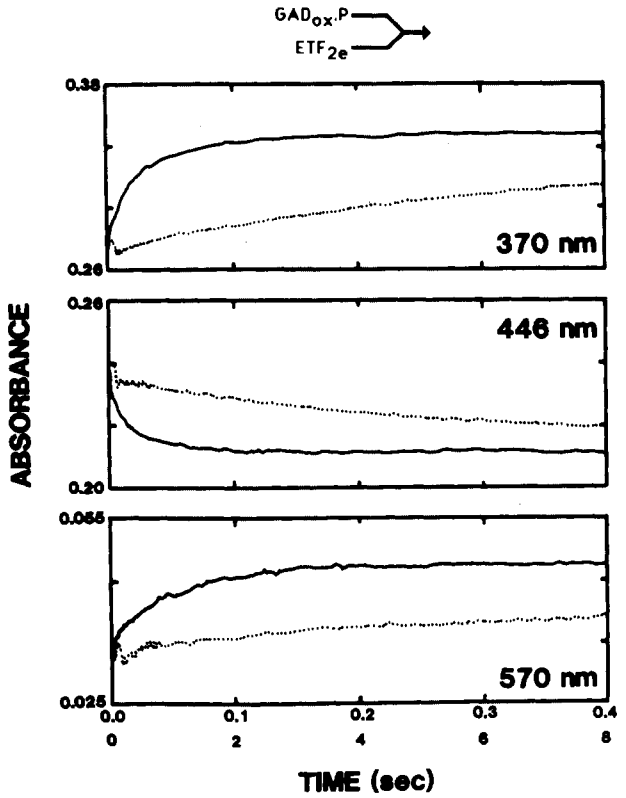

FIGURE 9: Absorbance vs. time traces following the reaction of oxidized general acyl-CoA dehydrogenase–octenoyl-CoA complex with fully reduced ETF. GAD_{ox}·P and ETF_{2e} were prepared as described under Materials and Methods. Equal volumes of GAD_{ox}·P (20 μM) and ETF_{2e} (20 μM) were mixed in a stopped-flow spectrophotometer under anaerobic conditions in 20 mM KP_i, pH 7.6, 3 °C. In each panel, the time courses of the absorbance changes over 0.4 (···) and 8 s (—) are displayed. Measurements were made in a 2-cm path-length cell. The wavelength being monitored is indicated in each panel.

nm. The absorbance changes are small and multiphasic, but the faster phases are consistent with the proposed reaction for step 3. The rise at 570 nm reflects the formation of GAD_{2e}·P. Similarly, the rise at 470 nm is consistent with the positive extinction change for ETF_{2e}/ETF_{1e} being larger than the negative extinction change for GAD_{1e}·P/GAD_{2e}·P. The reverse situation exists at 390 nm. In all cases, these fast-phase absorbance changes extend over 4 s, having a $t_{1/2}$ of about 0.5 s. As such, they are 10-fold slower than the changes proposed for steps 1 and 2 and consistent with our proposed mechanism.

Reversal of step 3, the reaction of GAD_{2e}·P with ETF_{1e}, was also examined. This reaction was slow, with a $t_{1/2}$ value of about 1.5 s. The absorbance changes for this slow reaction were consistent with oxidation of GAD_{2e}·P to GAD_{1e}·P and reduction of ETF_{1e} to ETF_{2e}.

Step 4 was examined by reacting GAD_{ox}·P with ETF_{2e}. Figure 9 shows that the time course of this reaction extends over about 4 s primarily in a single phase. Slower, minor absorbance changes lasted to 80 s at some wavelengths. The $t_{1/2}$ value for the fast phase was about 0.25 s, which is more than 5-fold slower than either step 1 or 2 and consistent with Scheme I. It should be noted that the products from this reaction can in turn react via step 1 to form ETF_{ox} and GAD_{2e}·P. However, this reaction should be limited by the slower rate observed in step 4. The absorbance change at 370 nm was positive as expected for radical formation from both oxidized GAD and reduced ETF. At 446 nm the net change was negative, as expected, since the Δ extinction for GAD_{ox}·P going to GAD_{1e}·P is negative and larger than the countering positive displacement for ETF_{2e} going to ETF_{1e}. The rise at 570 nm was indicative of GAD_{ox}·P reduction.

Table II: pH Effects on the Equilibrium upon Mixing Equimolar Electron-Transferring Flavoprotein and Octanoyl-CoA-Reduced General Acyl-CoA Dehydrogenase[a]

pH[b]	% ETF_{ox} remaining
6.72	34
7.56	26
8.16	20
8.36	19

[a] ETF and dehydrogenase (10 μM each) were incubated in 20 mM phosphate buffer (pH 6.72 and 7.56) or in 20 mM Tris buffer (pH 8.16 and 8.36) at 3 °C. The amount of ETF_{ox} before and after the addition of 10 μM octanoyl-CoA was determined by fluorescence, with excitation at 435 nm and emission at 500 nm. ETF_{ox} emission was corrected for internal quenching and dilution. [b] pH measurements were made at 3 °C.

The companion reaction for step 4, GAD_{1e}·P vs. ETF_{1e}, is complicated by the fact that this combination of reactants will also generate GAD_{2e}·P and ETF_{ox} via step 1. In fact, a fast phase ($t_{1/2}$ of about 60 ms) was observed. A loss of absorbance at 370 nm, a rise in absorbance at 450 nm, and a rise in absorbance at 570 nm during this phase were all consistent with the conversion of GAD_{1e}·P and ETF_{1e} to GAD_{2e}·P and ETF_{ox}. The slower absorbance changes appeared to be biphasic ($t_{1/2}$ of about 0.4 s and $t_{1/2}$ of about 3 s). These changes involved a net loss of absorbance at all wavelengths, reflecting a complex electron distribution.

Summary of Scheme I. In summary, the results of our studies into the various reactions depicted in Scheme I support that model as the basis for electron transfer between general acyl-CoA dehydrogenase and ETF. The fastest reactions occur in steps 1 and 2. The $t_{1/2}$ values for these steps were measured at 20–60 ms, depending on the experimental conditions. Note that both steps are 5–10 fold faster than the subsequent reactions, steps 3 and 4. Values for $t_{1/2}$ for steps 3 and 4 appear to be about 0.25 to 0.5 s. Thus, reaction of GAD_{2e}·P with ETF_{ox} would initially yield ETF_{1e} as the primary ETF product, and in turn, ETF_{1e} may represent the immediate reductant of ETF–ubiquinone oxidoreductase.

pH Effects on the Equilibrium Mixture in the Presence of Octenoyl-CoA. The experiments described earlier indicate that the reaction of GAD_{2e}·P with equimolar ETF_{ox} results in an equilibrium in which approximately one-fourth of the starting concentration of ETF_{ox} remains. Reinsch et al. (1980) performed similar experiments at pH 8.5, 25 °C, and concluded that there was essentially no ETF_{ox} (as judged by fluorescence) at the end of the reaction. Thus, it appeared that the equilibrium was sensitive to pH. To test this possibility, we reacted equimolar GAD_{2e}·P and ETF_{ox} at various pH values and allowed the reaction to come to equilibrium. We indeed found that the percentage of ETF_{ox} fluorescence remaining was influenced by pH (Table II). As the pH was increased from 6.7 to 8.2, less fluorescence due to ETF_{ox} was found in the equilibrium mixture. The fluorescence of ETF_{ox} was unaffected by pH. However, the effect of pH was minor, and significant ETF_{ox} remained at pH 8.2. These results were seemingly inconsistent with those reported by Reinsch et al. (1980).

In quantitating their data, Reinsch et al. (1980) used the following extinction coefficients: GAD_{ox}, 11 300 M^{-1} cm^{-1} at 450 nm; GAD_{2e}·P, 0 M^{-1} cm^{-1} at 450 nm; ETF_{ox}, 11 300 M^{-1} cm^{-1} at 450 nm. These values have since been refined: GAD_{ox}, 15 400 M^{-1} cm^{-1} at 446 nm (Thorpe, et al., 1979); GAD_{2e}·P, 2900 M^{-1} cm^{-1} at 446 nm (see Figure 1); ETF_{ox}, 13 300 M^{-1} cm^{-1} at 436 nm (Gorelick et al., 1982). Recalculation of the data presented in Table I in the paper of Reinsch et al. using

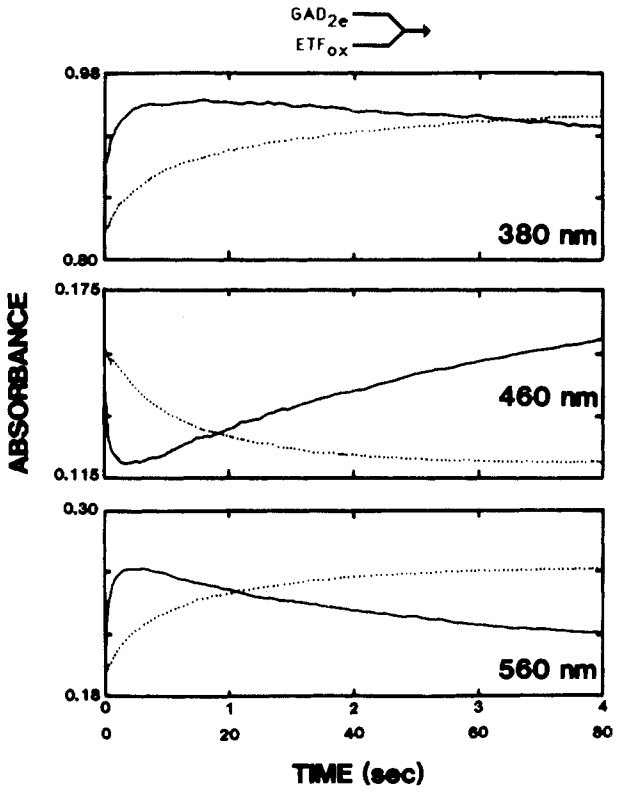

FIGURE 10: Absorbance vs. time traces following the reaction of fully reduced general acyl-CoA dehydrogenase with oxidized ETF. Conditions: GAD_{2e} and ETF_{ox} were prepared as described under Materials and Methods. Equal volumes of GAD_{2e} (20 μM) and ETF_{ox} (20 μM) were mixed in a stopped-flow spectrophotometer under anaerobic conditions in 20 mM KP_i, pH 7.6, 3 °C. In each panel, the time courses of the absorbance changes over 4 (···) and 80 s (—) are displayed. Measurements were made in a 2-cm path-length cell. The wavelength being monitored is indicated in each panel.

the newer values for the extinction coefficients indicates that 5–10% of the GAD remained reduced even in the presence of a 2–4-fold excess of ETF_{ox}. This strongly suggests the existence of an equilibrium such as we have described, even under their experimental conditions.

Reduction of ETF_{ox} by GAD_{2e} in the Absence of Product. Figure 10 depicts stopped-flow traces at 380, 460, and 560 nm when equimolar amounts of photochemically reduced general acyl-CoA dehydrogenase and oxidized ETF were mixed in a stopped-flow spectrophotometer. The analogous experiments with substrate-reduced dehydrogenase are shown in Figure 4. The two main phases evident in Figure 10 correspond to $t_{1/2}$ times of 0.6 and 60 s, more than 10-fold slower than those observed in the presence of product.

The appearance of the blue semiquinone form of the dehydrogenase in the faster phase was indicated by the rise in absorbance at 560 nm. Concomitant formation of the red ETF radical was suggested by the rise in absorbance at 380 nm. These changes were accompanied by a net loss in absorbance at 460 nm, reflecting the fact that the negative absorbance change which occurs when ETF_{ox} is reduced to ETF_{1e} is larger than the positive change found when GAD_{2e} is oxidized to GAD_{1e}. This mixture transformed, in the slow phase, to reduced ETF and oxidized dehydrogenase, resulting in a loss of absorbance at 380 nm, a rise at 460 nm, and a loss at 560 nm. These latter changes are conveniently seen by taking difference spectra between a spectrum recorded after 3 s (a time close to the end of the fast phase) and spectra collected at intervals up to several minutes after mixing (see Figure 11). The characteristic-resolved profile of the blue dehydrogenase

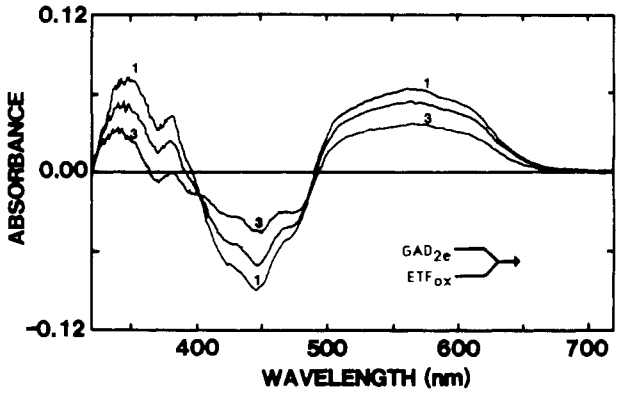

FIGURE 11: Difference spectra representing the slow phase absorbance changes following the reaction of fully reduced general acyl-CoA dehydrogenase with oxidized ETF in the absence of octenoyl-CoA. Conditions are the same as in Figure 10. Spectra were taken in the stopped-flow spectrophotometer at 60 nm/s. The first spectrum was begun 3 s after mixing, by which time the first phase change was complete. The traces represent difference spectra obtained by subtracting, from the 3-s spectrum, the spectra obtained at 5 (trace 1), 2.5 (trace 2), and 1.0 min (trace 3).

semiquinone in the 500–650 nm region (note the peak at 555 nm and the shoulder at about 615 nm) is clearly evident (Thorpe et al., 1979). The absorbance changes at the end of the fast phase in Figure 10 are consistent with the formation of about 70% blue dehydrogenase semiquinone and a similar level of ETF red radical (see Table I for extinction coefficients and isosbestics wavelengths).

These results demonstrate the sizable effects exerted by octenoyl-CoA on interflavin electron-transfer reactions between pig kidney general acyl-CoA dehydrogenase and electron-transferring flavoprotein. First, by preferential binding to the reduced dehydrogenase, octenoyl-CoA renders the enzyme a thermodynamically weaker reductant of ETF. This leads to the equilibrium observed in static and stopped-flow experiments. In vivo, ETF semiquinone would be rapidly oxidized with delivery of reducing equivalents to ETF–ubiquinone oxidoreductase at the inner mitochondrial membrane surface, thereby assuring that reducing equivalents would be passed down the respiratory chain. Secondly, octenoyl-CoA binding to the dehydrogenase significantly accelerates the rate of electron transfer to ETF. Thus, in the absence of product, the two main reductive phases have half-times of approximately 0.6 and 60 s at 3 °C, compared to 0.03 and 1 s in the presence of octenoyl-CoA. These data are consistent with an ordered ternary mechanism deduced from steady-state kinetic experiments, in which enoyl-CoA product dissociates last (McKean et al., 1979). Bound product assures rapid delivery of both dehydrogenase electrons to ETF molecules, whereas if enoyl-CoA were to dissociate prior to reoxidation, both electron-transfer steps would be slower than overall turnover.

What is the molecular basis for the enhanced electron-transfer rates when substrate-reduced dehydrogenase is employed? One possibility is that conformational changes induced upon reduction of the dehydrogenase with substrate allow a more effective alignment of flavin centers for electron transfer in the absence of product. A second possibility is that the donor flavin needs to be anionic for rapid reduction of ETF (Mizzer & Thorpe, 1982). In the absence of bound acyl-CoA substrates or products, both the semiquinone and probably the dihydroflavin form of the dehydrogenase are in their protonated, neutral, forms (Mizzer & Thorpe, 1982; Thorpe & Massey, 1983). In contrast acyl-CoA substrates or products stabilize the red anionic dehydrogenase radical and probably the dihydroflavin anion form of the dehydrogenase (Mizzer

& Thorpe, 1982; Thorpe & Massey, 1983; Ghisla, 1984). It should also be noted that transfer of one electron from GAD_{2e}·P to ETF_{ox} generates anionic flavin species on both proteins. Conceivably, electrostatic repulsion between these flavins could be utilized to promote dissociation of the GAD_{1e}·P·ETF_{1e} complex allowing binding of a second ETF_{ox} molecule prior to the second rapid interflavin electron transfer step (Scheme I). This scheme would be consistent with ETF radical being the primary donor to the ETF–ubiquinone oxidoreductase, thus regenerating oxidized ETF. This could constitute the main switchpoint for two-electron to one-electron transfers involved in oxidation of fatty acids, several amino acids, and choline.

Registry No. Acyl-CoA dehydrogenase, 9027-65-0; octanoyl-CoA, 1264-52-4.

REFERENCES

Beaty, N. B., & Ballou, D. P. (1981) *J. Biol. Chem. 256*, 4611–4618.

Beckmann, J. D., & Frerman, F. E. (1983) *J. Biol. Chem. 258*, 7563–7569.

Beckmann, J. D., Frerman, F. E., & McKean, M. C. (1981) *Biochem. Biophys. Res. Commun. 102*, 1290–1294.

Beinert, H. (1963a) *Enzymes, 2nd Ed. 7*, 467–476.

Beinert, H. (1963b) *Enzymes, 2nd Ed. 7*, 447–466.

Beinert, H., & Frisell, W. R. (1962) *J. Biol. Chem. 237*, 2988–2990.

Bernert, J. T., & Sprecher, H. (1977) *J. Biol. Chem. 252*, 6736–6744.

Besrat, A., Polan, C. E., & Henderson, L. M. (1969) *J. Biol. Chem. 244*, 1461–1467.

Crane, F. L., & Beinert, H. (1956) *J. Biol. Chem. 218*, 717–731.

Entsch, B., Ballou, D. P., & Massey, V. (1976) *J. Biol. Chem. 251*, 2550–2563.

Feinberg, B. A., & Gustafson, W. G. (1982) in *Flavins and Flavoproteins* (Massey, V., & Williams, C. H., Jr., Eds.) pp 632–636, Elsevier/North-Holland, New York.

Fersht, A. (1977) *Enzyme Structure and Mechanism*, pp 163–164, W. H. Freeman, San Francisco.

Frerman, F. E., Mielke, D., & Huhta, K. (1980) *J. Biol. Chem. 255*, 2199–2202.

Frisell, W. R., Cronin, J. R., & Mackenzie, C. G. (1966) in *Flavins and Flavoproteins* (Slater, E. C., Ed.) pp. 386–390, Elsevier, Amsterdam.

Ghisla, S. (1984) in *Flavins and Flavoproteins* (Bray, R. C., Engel, P. C., & Mayhew, S. G., Eds.) pp 385–402, de Gruyter, Berlin.

Ghisla, S., Thorpe, C., & Massey, V. (1984) *Biochemistry 23*, 3154–3161.

Gibson, Q. H., & Milnes, L. (1964) *Biochem. J. 91*, 161–171.

Gibson, Q. H., Hastings, J. W., Weber, G., Duane, W., & Massa, J. (1966) in *Flavins and Flavoproteins* (Slater, C., Ed.) pp 341–366, Elsevier, Amsterdam.

Gorelick, R. J., & Thorpe, C. (1984) in *Flavins and Flavoproteins* (Bray, R. C., Engel, P. C., & Mayhew, S. G., Eds.) pp 761–764, de Gruyter, Berlin.

Gorelick, R. J., Mizzer, J. P., & Thorpe, C. (1982) *Biochemistry 21*, 6936–6942.

Hall, C. L., & Kamin, H. (1975) *J. Biol. Chem. 250*, 3476–3486.

Hall, C. L., & Lambeth, J. D. (1980) *J. Biol. Chem. 255*, 3591–3595.

Hall, C. L., Lambeth, J. D., & Kamin, H. (1979) *J. Biol. Chem. 254*, 2023–2031.

Husain, M., Stankovich, M. T., & Fox, B. G. (1984) *Biochem. J. 219*, 1043–1047.

Ikeda, Y., & Tanaka, K. (1983) *J. Biol. Chem. 258*, 9477–9487.

Lau, E. P., Haley, B. E., & Barden, R. E. (1977) *Biochemistry 16*, 2581–2585.

Massey, V., & Hemmerich, P. (1978) *Biochemistry 17*, 9–17.

McKean, M. C., Frerman, F. E., & Mielke, D. M. (1979) *J. Biol. Chem. 254*, 2730–2734.

Mizzer, J. P., & Thorpe, C. (1981) *Biochemistry 20*, 4965–4970.

Mizzer, J. P., & Thorpe, C. (1982) in *Flavins and Flavoproteins* (Massey, V., & Williams, C. H., Jr., Eds.) pp 637–640, Elsevier/North-Holland, New York.

Moore, E. G., Cardemil, E., & Massey, V. (1978) *J. Biol. Chem. 253*, 6413–6422.

Noda, C., Rhead, W. J., & Tanaka, K. (1980) *Proc. Natl. Acad. Sci. U.S.A. 77*, 2646–2650.

Reinsch, J. W., Feinberg, B. A., & McFarland, J. T. (1980) *Biochem. Biophys. Res. Commun. 94*, 1409–1416.

Ruzicka, F. J., & Beinert, H. (1977) *J. Biol. Chem. 252*, 8440–8445.

Steenkamp, D. J., & Husain, M. (1982) *Biochem. J. 203*, 707–715.

Thorpe, C., & Massey, V. (1983) *Biochemistry 22*, 2972–2978.

Thorpe, C., Matthews, R. G., & Williams, C. H., Jr. (1979) *Biochemistry 18*, 331–337.

Williams, C. H., Jr., Arscott, L. D., Matthews, R. G., Thorpe, C., & Wilkinson, K. D. (1979) *Methods Enzymol. 62*, 185–198.